American Mineralogist, Volume 66, pages 87–99, 1981

High-grade metamorphic Archean banded iron-formations, Western Australia: assemblages with coexisting pyroxenes ± fayalite

MARTIN J. GOLE[1] AND CORNELIS KLEIN

Department of Geology, Indiana University
Bloomington, Indiana 47405

Abstract

At Heaney's Find, Meier's Find, and Queen Victoria Rocks in the greenstone belt terrain (~2.6–2.7 Gyr) of the Yilgarn Block of Western Australia, banded iron-formations have been regionally metamorphosed. The primary metamorphic assemblages in the iron-formations contain quartz, grunerite, clinopyroxene, orthopyroxene, magnetite, and minor hornblende and pyrrhotite. Fayalite is also present at Heaney's Find and Queen Victoria Rocks. Fe-shales interbanded with the iron-formations contain hornblende, almandine, and minor biotite, plagioclase, ilmenite, magnetite, and pyrrhotite. Smooth, curved grain boundaries between various combinations of the above minerals suggest that they are equilibrium assemblages. Actinolite and some grunerite with ragged boundaries against other minerals are interpreted as having formed after the primary assemblages. Asbestiform grunerite, ragged magnetite, and greenalite are retrograde. Based on (a) two-pyroxene geothermometry, (b) olivine–orthopyroxene geothermometry, and (c) the absence of evidence for the crystallization of pigeonite, the peak metamorphic temperature is estimated to have been 670 ± 50°C. Using Smith's (1971) quartz–olivine–orthopyroxene geobarometer, the composition of orthopyroxene coexisting with fayalite + quartz in the iron-formation assemblages indicates that the pressure during metamorphism was 3–5 kbar. A somewhat lower pressure, as indicated by experimental data for the quartz + olivine → orthopyroxene reaction (Bohlen *et al.* 1978), is also consistent with the geology of these three areas.

Introduction

Metamorphosed banded iron-formations from three locations, Meier's Find, Heaney's Find, and Queen Victoria Rocks (Fig. 1) in the greenstone belt terrain of the Eastern Goldfields Province of the Yilgarn Block, Western Australia (Rb–Sr isotopic age of 2.6–2.7 Gyr; Arriens, 1971) contain coexisting ortho- and clinopyroxene. Two of these occurrences contain fayalite ± quartz as well. Comparison of the compositions of coexisting orthopyroxene, clinopyroxene, and fayalite with experimental data allows an estimation of metamorphic temperature and pressure. These results are of particular interest, as estimates of pressure during high-grade metamorphism of the volcanogenic supracrustal (greenstone) belts in the Yilgarn Block are uncommon, due to a scarcity within the greenstone successions of pressure-sensitive metamorphic assemblages such as metapelites.

Assemblages containing orthopyroxene, clinopyroxene, and fayalite are uncommon in metamorphosed iron-formations. Such assemblages have been reported from the highly metamorphosed portions of the Biwabik (Bonnichsen, 1969, 1975) and Gunflint Iron Formations (Simmons *et al.,* 1974) where they are the result of contact metamorphism by the Duluth Complex, and in iron-formations metamorphosed by the Nain Complex in Labrador (Berg, 1977). Such assemblages contain evidence of inverted pigeonite whereas those from the Yilgarn Block do not. Fayalite-bearing assemblages lacking orthopyroxene have been reported from the moderately metamorphosed portions of the Biwabik (Morey *et al.,* 1972), and Gunflint Iron Formations (Floran and Papike, 1978), the Negaunee Iron Formation (Haase and Klein, 1978), and from iron-formations at Koolanooka in the Yilgarn Block (Baxter, 1965; Gole, 1980a). Such orthopyroxene-free assemblages provide few constraints for estimating metamorphic pressure. Fayalite–orthopyroxene-bearing assem-

[1]Present address: Department of Geology, Georgia State University, University Plaza, Atlanta, Georgia 30303.

0003–004X/81/0102–0087$02.00

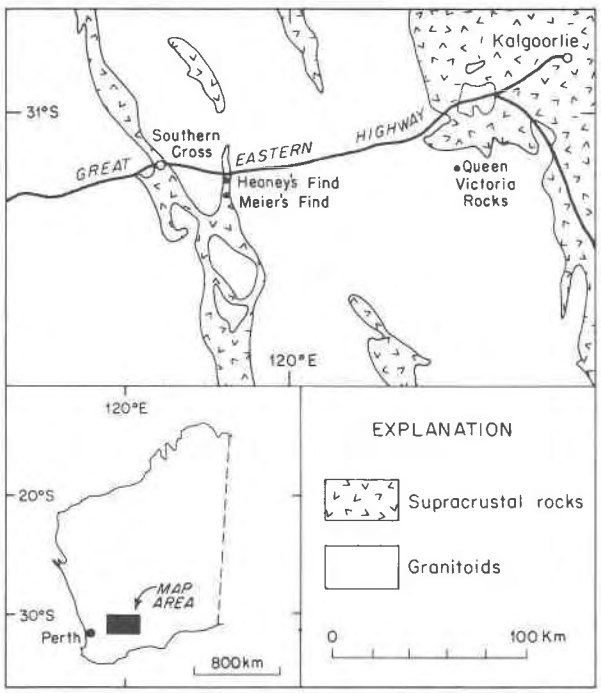

Fig. 1. Map of part of the Eastern Goldfields Province of the Yilgarn Block, Western Australia, showing the distribution of supracrustal rocks (greenstone belts) and granitoids and the locations of Heaney's Find, Meier's Find, and Queen Victoria Rocks.

blages from lithologies other than iron-formations are briefly reviewed in Jaffe *et al.* (1978).

Geologic setting

The assemblages in the banded iron-formation from Heaney's Find and Meier's Find have previously been described by Miles (1943, 1946a, b). Samples for this study were obtained from two diamond drill holes at Heaney's Find (sample 4 from D.D.H. 3, others from D. D.H. 1; Miles, 1946a) and from one diamond drill hole at Meier's Find (D.D.H. 2; Miles, 1946a). The diamond drill holes at Heaney's Find are 140 m apart and approximately equidistant from a poorly exposed granitoid–greenstone contact. At both Heaney's Find and Meier's Find the diamond drill holes are located near the contact of a 2–4km-wide greenstone belt and a large granitoid pluton. The greenstone belt represents the eastern limb of a regional-scale anticline with the granitoid occupying the core (Fig. 1). Miles (1946a,b) described the local geology at both locations.

At Heaney's Find intrusive granitoids crop out 500 m west of the banded iron-formations. The iron-formations are steeply dipping, 5–20 m thick, and occur within a sequence of hornblende + plagioclase + augite ± biotite and tremolite + anthophyllite ± talc schists. Relict pillows within the schists indicate that they are probably the metamorphosed and deformed equivalents of mafic and ultramafic volcanics, respectively. Intercalated with these schists are thin bands of argillaceous metasediments. The area has been intruded by numerous pegmatitic dikes.

The local geology at Meier's Find is very similar to that of Heaney's Find except for the lack of ultramafic rocks (Miles, 1946a). At Meier's Find, the banded iron-formation is locally in contact with cross-cutting granitoid bodies, and granitoid was encountered at depths of 40–60 m in several diamond drill holes (Miles, 1946a).

At Queen Victoria Rocks (Fig. 1), a small (probably 3–6 km^2) outlier of highly metamorphosed mafic, ultramafic, and metasedimentary rocks occurs within the granitoid. Outcrop is almost non-existent, and the relationship between rock types is not clear.

Heaney's Find, Meier's Find, and Queen Victoria Rocks are all in the dynamic-style high-grade metamorphic domain mapped by Binns *et al.* (1976). As such, the metamorphic assemblages at these localities are part of a regionally extensive metamorphic environment that extends well away from granitoid contacts. Contact metamorphism related to granitoid emplacement, which in places is superimposed on the regional metamorphic pattern, forms distinct, narrow aureoles of fine-grained hornfelses (Binns *et al.*, 1976, p. 306). The assemblages at Heaney's Find, Meier's Find, and Queen Victoria Rocks do not have hornfelsic textures, but instead show textures similar to those in lithologies in the high-grade domain well within the greenstone belts (R. A. Binns, personal communication, 1980). Thus, despite the close spatial relationship between the greenstone lithologies and the intrusive granitoids at these localities, the metamorphic assemblages are not the result of contact metamorphism. Binns *et al.* (1976) [see also Archibald *et al.* (1978)] suggest that the heat source responsible for the regional metamorphic pattern also caused the generation of the intrusive granitoids by reactivating granitoid gneisses which formed the basement to the greenstone cover (Archibald and Bettenay, 1977).

Analytical methods

Analyses of bulk samples were obtained by X-ray fluorescence spectroscopy, except that Na was analyzed by atomic absorption spectroscopy, FeO by titration against potassium dichromate, H_2O and CO_2

by gravimetric means, and S with a Leco furnace. Electron microprobe analyses were made on four samples from Heaney's Find, four from Meier's Find, and eight from Queen Victoria Rocks. These samples contain the most diverse assemblages collected. Analyses were made on a 3-spectrometer Etec Autoprobe, with the data reduction procedure of Bence and Albee (1968). Alpha factors used were those of Albee and Ray (1970). Analyses with the same sample number but different letters were obtained from different mesobands or Fe-shale bands within the same sample. The majority of the analyses in Tables 3 to 7 are averages of 3 to 6 individual analyses, as are the points in Figures 3, 4, and 5.

Lithologies

Two Fe-rich rock types, banded iron-formation and Fe-shale, occur at Heaney's Find, Meier's Find, and Queen Victoria Rocks. Banded iron-formation generally consists of alternating 2–30 mm thick mesobands, although some iron-formation is massive. Successive mesobands are distinguished by (a) different mineral assemblages, (b) differences in the relative proportions of minerals, (c) the presence or absence of microbands, and (d) different spacing between microbands. Microbanding in these highly metamorphosed iron-formations is uncommon and is best preserved in quartz–magnetite-rich assemblages which, although they are recrystallized, show little or no reaction between minerals (Fig. 2a). In iron-silicate- and originally carbonate-rich mesobands, metamorphic reactions and recrystallization have destroyed or severely modified earlier structures.

The bulk compositions of the banded iron-formations (Table 1) are characterized by SiO_2 + Fe_2O_3 + FeO totals over 90 wt. percent, by low but significant (<4 wt. percent) contents of MgO and CaO, and by variable but small Al_2O_3 contents. Despite their low concentrations, these minor components have an important effect on assemblages in the iron-formations. Other components generally occur in trace amounts (<0.31 wt. percent).

Fe-shale occurs as 1–30 cm-thick bands within the iron-formation. These bands are massive, and minerals are generally evenly distributed throughout them. In hand specimen, they are distinguishable from banded iron-formation by their brownish-green color, which is a result of the dark green hornblende ± almandine ± biotite they contain. The bulk compositions of Fe-shales are highly variable, although they have some common chemical characteristics. They are Fe-rich, containing more than 20 wt. percent total Fe, and their minor components, particularly Al_2O_3 and TiO_2, are significantly higher than in the banded iron-formations (Table 1). The very low metamorphic-grade equivalents of the Fe-shales are very fine-grained and finely laminated. These essentially unmetamorphosed Fe-shales contain chamosite or chlorite, stilpnomelane, carbonate, magnetite, py-

Table 1. Bulk chemical analyses of iron-formations and Fe-shales. Analyses are from Tables 2 and 3 of Gole (1980b)

	Banded iron-formation			Fe-shale		
	2	12	15	4	13	14
SiO_2	62.78	40.84	47.27	36.75	42.52	41.43
TiO_2	0.00	0.00	0.00	0.42	0.64	0.45
Al_2O_3	0.08	0.14	1.60	8.09	12.10	14.70
Fe_2O_3	16.61	3.73	25.45	14.03	6.68	5.84
FeO	14.68	48.58	20.68	19.75	23.22	22.67
MnO	0.31	0.15	0.06	0.12	0.22	1.42
MgO	0.99	3.70	2.57	7.44	8.47	2.09
CaO	3.63	1.27	0.95	9.41	3.75	7.35
Na_2O	0.05	0.04	0.05	0.66	0.53	0.14
K_2O	0.01	0.02	0.01	0.94	0.49	1.51
H_2O^+	0.16	0.86	0.41	1.25	1.18	1.47
H_2O^-	0.06	0.03	0.02	0.09	0.11	0.25
P_2O_5	0.11	0.11	0.15	0.08	0.08	0.07
CO_2	-	-	-	-	-	0.37
S	0.02	0.04	0.00	0.22	0.00	0.00
-O=S	0.01	0.02	0.00	0.11	0.00	0.00
Total	99.48	99.49	99.22	99.13	99.99	99.76
Total Fe	23.02	40.37	33.88	25.16	22.73	21.70
Fe^{3+}/Fe^{2+}	1.02	0.07	1.11	0.66	0.26	0.23

Table 2. Summary of assemblages in iron-formations and Fe-shales

Sample No.	Catalog No.**	Assemblage
		Heaney's Find
1A	20839	ferroaug-eul-grun-fay-mag-hbld
1B	20839	ferroaug-grun-eul-qtz-fay-(mag)-(po)-(mag*)-(green*)
2	20841	qtz-mag-grun-fay-(po)
3	20843	qtz-ferrosal-grun-fay-mag-(grun*)-(mag*)
4A	20854	hbld-biot-alm-qtz-plag(An36)-(zircon)
4B	20854	hbld-alm-mag-po-(marcasite*)
4C	20854	ferroaug-eul-grun-fay-hbld-qtz-mag-(po)
4D	20854	ferroaug-fay-grun-hbld-mag-(po)-(mag*)
		Meier's Find
5	20844	alm-hbld-ferrosal-mag-(ilm)
6	20845	grun-ferroaug-eul-mag
7	20850	ferrosal-grun-fact-mag-(po)-(cpy)
8	*20851*	*qtz-biot-cumm-plag(An52)*
		Queen Victoria Rocks
9	84979	cumm-ferroaug-ferrohyp-mag-qtz-(po)-(cpy)
10	84985	grun-ferroaug-eul-(qtz)-(po)-(mag*)-(green*)
11	84986	grun-ferroaug-fay-hbld-(qtz)-(grun*)-(mag*)
12A	84987	fay-grun-qtz-ferroaug-mag
12B	84987	ferroaug-eul-fay-qtz-grun-(po)-(mag)
13A	84990	ferroaug-eul-grun-qtz-hbld-mag
13B	84990	hbld-ferrosal-grun-(po)
14	84991	hbld-alm-cumm-biot-mag-ilm
15	84992	qtz-mag-grun
16	*84998*	*qtz-plag(An34)-biot-hbld*

Mineral abbreviations

alm = almandine	ferrosal = ferrosalite
biot = biotite	green = greenalite
cpy = chalcopyrite	grun = grunerite
cumm = cummingtonite	hbld = hornblende
eul = eulite	ilm = ilmenite
fay = fayalite	mag = magnetite
fact = ferroactinolite	plag = plagioclase
ferroaug = ferroaugite	po = pyrrhotite
ferrohyp = ferrohypersthene	qtz = quartz

***Catalog numbers in the collection of the Department of Geology, University of Western Australia.*

*Minerals are listed in decreasing relative abundance. Parentheses means trace amount. * signifies retrograde mineral. Assemblages in italics represent pelitic metasediments.*

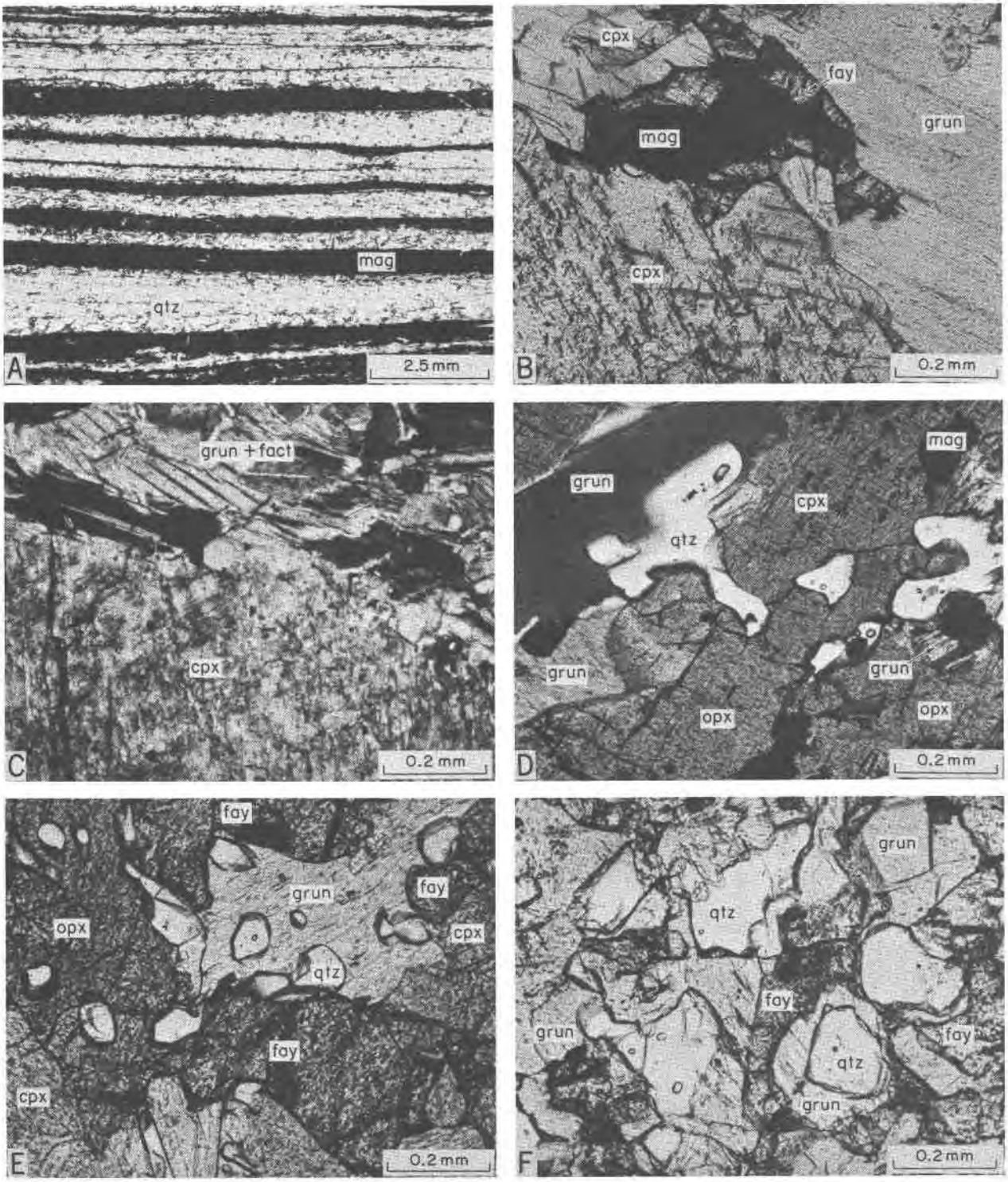

Fig. 2. Textures and structures in iron-formations. Mineral abbreviations are listed in Table 2. (A) Thin mesobands composed of magnetite and quartz with minor grunerite. Some of the quartz-rich mesobands contain poorly-defined microbands. Queen Victoria Rocks, sample 15. Plane polarized light. (B) An aggregate of equant magnetite grains rimmed by fayalite in a grunerite–ferroaugite-rich assemblage. Fayalite contains inclusions of fine-grained magnetite along fractures and some grain boundaries. Ferroaugite (cpx) contains fine-grained ragged inclusions of ferroactinolite. Heaney's Find, sample 1A. Plane polarized light. (C) A large ferrosalite grain

rite, pyrrhotite, quartz or chert, potassium feldspar, ilmenite, and carbonaceous material, and are commonly interbanded with both Archean and Proterozoic banded iron-formations (Gole, 1980b).

Assemblages

The iron-formation assemblages at Heaney's Find and Queen Victoria Rocks are very similar (Table 2), with clinopyroxene, orthopyroxene, grunerite, quartz, minor magnetite, and hornblende the most common constituents. Fayalite-bearing assemblages are uncommon and may or may not contain orthopyroxene or quartz. Pyrrhotite is present in trace amounts in many assemblages. Similar assemblages occur at Meier's Find, although orthopyroxene is uncommon and fayalite is absent. Magnetite is not a major constitutent of the iron-formations at any of the locations, and is generally restricted to quartz-rich Fe-silicate-poor assemblages. The minerals in Fe-silicate-rich mesobands are evenly distributed, with the following exceptions: (a) where quartz occurs in aggregates in some mesobands defining a crude layering roughly parallel to mesoband contacts, (b) where magnetite is rimmed by fayalite as in samples 1A and 1B (Fig. 2b), and (c) where retrograde minerals are present. Nevertheless, the prograde minerals listed in Table 2 are in mutual contact somewhere within a small area of a thin section.

Fe-shale bands are composed predominantly of hornblende and almandine and may contain variable amounts of biotite, ferrosalite, grunerite, and ferroactinolite. Quartz, andesine, fayalite, magnetite, ilmenite, and pyrite or pyrrhotite are minor minerals and apatite and zircon are trace constituents. The minerals are evenly distributed throughout Fe-shale bands except in one hornblende-rich band where grunerite occurs as rims around fayalite.

Based on textural relations, the following minerals are clearly not part of the high-grade metamorphic assemblages: (a) very fine-grained asbestiform grunerite that projects into quartz grains along mutual contacts with Fe-silicate, (b) fine-grained, ragged magnetite distributed along fractures, cleavages and grain boundaries in many assemblages, and (c) greenalite, which occurs in veinlets.

Quartz is abundant in most samples of iron-formation but occurs in small amounts or is absent in most fayalite-bearing assemblages and Fe-shale bands. In quartz-rich mesobands, quartz aggregates form thin laminae separated by laminae of Fe-silicates or magnetite or both. The laminae probably represent relict microbanding.

Orthopyroxene occurs as coarse to very coarse anhedral grains (0.2–10 mm and locally >2 cm in diameter). The large grains contain inclusions of magnetite, quartz, sulfides and, less commonly, hornblende and ragged fine-grained grunerite. Grain boundaries are generally smooth and curved against other prograde minerals (Figs. 2d and e), except in some samples where grain boundaries with grunerite are somewhat irregular. Extremely fine (<1–2 μm) exsolution lamellae of calcic pyroxene parallel to (100) are visible in many grains. The $Fe^{2+}/(Fe^{2+}+Mg+Mn)$ ratio of orthopyroxene ranges from 0.762 to 0.831 (Table 3, Figure 3). Within a mesoband, compositions are similar regardless of adjacent minerals. Ca values are relatively uniform which suggests that the exsolution lamellae have not biased the electron probe analyses towards either the composition of the host or the exsolution lamellae. Orthopyroxenes from Heaney's Find and Meier's Find have considerably higher MnO contents (1.34–2.27 wt. percent) than those from Queen Victoria Rocks (0.18–0.51 wt. percent; see Table 3, Fig. 4). Estimated Fe_2O_3 values are low and variable and may not reflect the actual ferric contents of the pyroxenes.

Clinopyroxene is texturally very similar to orthopyroxene. In some assemblages clinopyroxene contains abundant inclusions of fine-grained actinolite, ragged grunerite, and minute grains of magnetite (Fig. 2c), whereas coexisting orthopyroxene is generally inclusion-free. Exsolution lamellae parallel to (100) are common and are more pronounced than those in orthopyroxene. Exsolution lamellae parallel to other crystallographic directions are rare, however. For the averaged analyses of clinopyroxene coexisting with orthopyroxene (Table 3), the 'Wo' content, defined as the ratio Ca/(Ca+Fe+Mn+Mg), ranges from 0.427 to 0.439, although the range between single analyses is greater, reflecting the presence of

with an intergrowth of grunerite and ferroactinolite along its boundary. Ferrosalite (cpx) contains inclusions of very fine-grained magnetite and ragged ferroactinolite. Meier's Find, sample 7. Doubly polarized light. (D) Coexisting ferroaugite (cpx), eulite (opx), grunerite, quartz, and magnetite. Queen Victoria Rocks, sample 13A. Doubly polarized light. (E) Coexisting fayalite, eulite (opx), ferroaugite (cpx), grunerite, and quartz. Note the smooth, curved grain boundaries between all minerals. Queen Victoria Rocks, sample 12B. Plane polarized light. (F) Fayalite–grunerite–quartz assemblage in which grunerite mantles fayalite grains so that quartz and fayalite are not in contact. Grunerite–quartz boundaries are somewhat angular. Heaney's Find, sample 3. Plane polarized light.

Table 3. Representative electron microprobe analyses of coexisting and single pyroxenes in iron-formation and Fe-shales

	Heaney's Find							Meier's Find			Queen Victoria Rocks					
	4C		1B		1A		3	6		7	12B		9		12A	13B
wt%	OPX	CPX	OPX	CPX	OPX	CPX	CPX	OPX	CPX	CPX	OPX	CPX	OPX	CPX	CPX	CPX
SiO_2	46.83	49.12	47.24	49.60	48.40	50.50	48.83	47.30	50.10	50.10	47.00	49.20	49.27	51.17	49.40	50.70
TiO_2	0.00	0.00	0.00	0.03	0.01	0.00	0.00	0.00	0.00	0.04	0.00	0.02	0.00	0.02	0.04	0.04
Al_2O_3	0.27	0.47	0.16	0.41	0.22	0.34	0.12	0.10	0.13	0.10	0.27	0.28	0.18	0.25	0.26	0.06
FeO*	44.68	24.60	44.36	24.30	42.58	22.80	25.07	43.50	23.70	21.40	45.90	24.60	39.63	18.65	24.70	17.10
MnO	2.27	1.06	1.99	0.92	1.62	0.78	0.94	1.34	0.69	0.68	0.18	0.12	0.51	0.27	0.09	0.23
MgO	4.70	4.33	4.77	4.67	6.54	5.78	3.85	5.83	5.39	5.57	5.13	4.90	10.18	8.61	4.43	7.98
CaO	0.89	19.85	0.95	20.10	0.96	20.57	20.50	1.04	19.80	21.90	0.90	20.20	0.80	20.97	20.70	23.20
Na_2O	0.00	0.21	0.03	0.09	0.06	0.03	0.12	0.00	0.08	0.00	0.00	0.09	0.00	0.02	0.05	0.00
K_2O	0.00	0.00	0.00	0.00	0.00	0.01	0.00	0.00	0.00	0.00	0.00	0.00	0.00	0.00	0.00	0.00
Sum	99.64	99.64	99.50	100.12	100.39	100.81	99.43	99.11	99.89	99.79	99.38	99.41	100.65	99.96	99.67	99.31
Fe_2O_3**	0.42	1.18	0.00	0.43	0.00	0.00	0.50	0.00	0.00	0.00	0.20	0.63	0.28	0.00	0.37	0.00
FeO	44.30	23.54		23.91			24.62				45.72	24.03	39.38		24.37	
Total	99.68	99.62		100.16			99.48				99.40	99.47	100.68		99.71	
	ions on the basis of 6 oxygens															
Si	1.985	1.979	2.000	1.986	2.002	1.993	1.984	1.997	2.002	1.995	1.990	1.983	1.989	1.994	1.989	1.991
Al	0.013	0.021	0.000	0.014	0.000	0.007	0.006	0.003	0.000	0.005	0.010	0.013	0.009	0.006	0.011	0.003
Σ	1.998	2.000	2.000	2.000	2.002	2.000	1.990	2.000	2.002	2.000	2.000	1.996	1.998	2.000	2.000	1.994
Al	0.000	0.001	0.008	0.006	0.011	0.009	0.000	0.002	0.006	0.000	0.004	0.000	0.000	0.005	0.001	0.000
Ti	0.000	0.000	0.000	0.001	0.000	0.000	0.000	0.000	0.000	0.001	0.000	0.001	0.000	0.001	0.001	0.001
Fe^{3+}	0.013	0.036	0.000	0.013	0.000	0.000	0.015	0.000	0.000	0.000	0.006	0.019	0.009	0.000	0.011	0.000
Fe^{2+}	1.570	0.793	1.571	0.801	1.473	0.753	0.837	1.536	0.792	0.713	1.619	0.810	1.329	0.608	0.820	0.561
Mn	0.082	0.036	0.071	0.031	0.057	0.026	0.032	0.048	0.023	0.023	0.006	0.004	0.017	0.009	0.003	0.008
Mg	0.297	0.260	0.301	0.279	0.403	0.340	0.233	0.367	0.321	0.331	0.324	0.294	0.612	0.500	0.266	0.467
Ca	0.040	0.857	0.043	0.863	0.043	0.870	0.893	0.047	0.848	0.934	0.041	0.872	0.038	0.876	0.893	0.976
Na	0.000	0.016	0.002	0.007	0.005	0.002	0.009	0.000	0.006	0.000	0.000	0.007	0.000	0.002	0.004	0.000
Σ	2.002	1.999	1.996	2.001	1.992	2.000	2.019	2.000	1.996	2.002	2.000	2.007	2.005	2.001	1.999	2.013

*All Fe as FeO. **Fe_2O_3 estimated by the method of Papike et al. (1974). Assemblages listed in Table 2.

exsolution lamellae. The 'Wo' content of clinopyroxenes from orthopyroxene-free assemblages tends to be larger than this range with the exception of one sample (Fig. 3, no. 4D), where exsolution lamellae may be present. Clinopyroxenes from Fe-shale assemblages (Fig. 3, samples 5 and 13B) have relatively high 'Wo' contents compared to those from banded iron-formations. Clinopyroxenes have the lowest Mn contents (Fig. 4) and lowest Fe/(Fe+Mg) ratios of any of the Fe–silicates in the assemblages. Estimated Fe_2O_3 contents are variable and are, on the average, slightly higher than those in orthopyroxene (Table 3).

Amphiboles may form up to 40 percent of the iron-formations and as much as 100 percent of the Fe-shales. The iron-formation assemblages contain grunerite with minor hornblende and generally only trace amounts of actinolite, whereas Fe-shale assemblages are dominated by hornblende (Table 2). Poikiloblastic grains of grunerite up to 0.5 cm long enclose quartz, pyroxene, fayalite, magnetite, and hornblende. Most grunerite, however, occurs as interlocking tabular grains. The poikiloblastic and many of the tabular grunerite grains have smooth contacts with adjacent minerals and appear to be part of the high-grade assemblage (Figs. 2b, d, and e). In a few samples (particularly no. 3), grunerite has angular boundaries, especially against quartz, and occurs as rims between quartz and fayalite (Fig. 2f), which suggests that this grunerite may be paragenetically later than most of the assemblage. There is, however, no clear-cut textural distinction between these later grunerites and the grunerite that is part of the high-grade assemblage. Most actinolite occurs late in the paragenetic sequence and is closely associated with clinopyroxene (Fig. 2c). Similar late-stage amphiboles have been described from the metamorphosed Biwabik and Gunflint Iron Formations (Bonnichsen, 1969, 1975; Morey *et al.*, 1972; Simmons *et al.*, 1974; Floran and Papike, 1978). Very fine-grained, fibrous to asbestiform grunerite is clearly later than the prograde assemblage, because it cuts across quartz grain boundaries and projects into quartz from orthopyroxene and other grunerite grains. This variety of grunerite is probably of retrograde origin, as noted by Bonnichsen (1969, 1975) and Immega and Klein (1976). Hornblende occurs as isolated polygonal grains within banded iron-formation assemblages and forms an almost monomineralic interlocking mosaic in many of the Fe-shale bands.

Members of the cummingtonite–grunerite series and actinolite are chemically simple and over 95% of their compositions can be represented in the Ca–Mg–(Fe+Mn) quadrilateral. One exception is cummingtonite from an Fe-shale band (Table 4, sample 14) that contains significant amounts of Al and Na. Although very fine exsolution lamellae are visible in most grains, CaO contents of grunerite are generally <1 wt. percent. The most Fe-rich grunerite occurs in

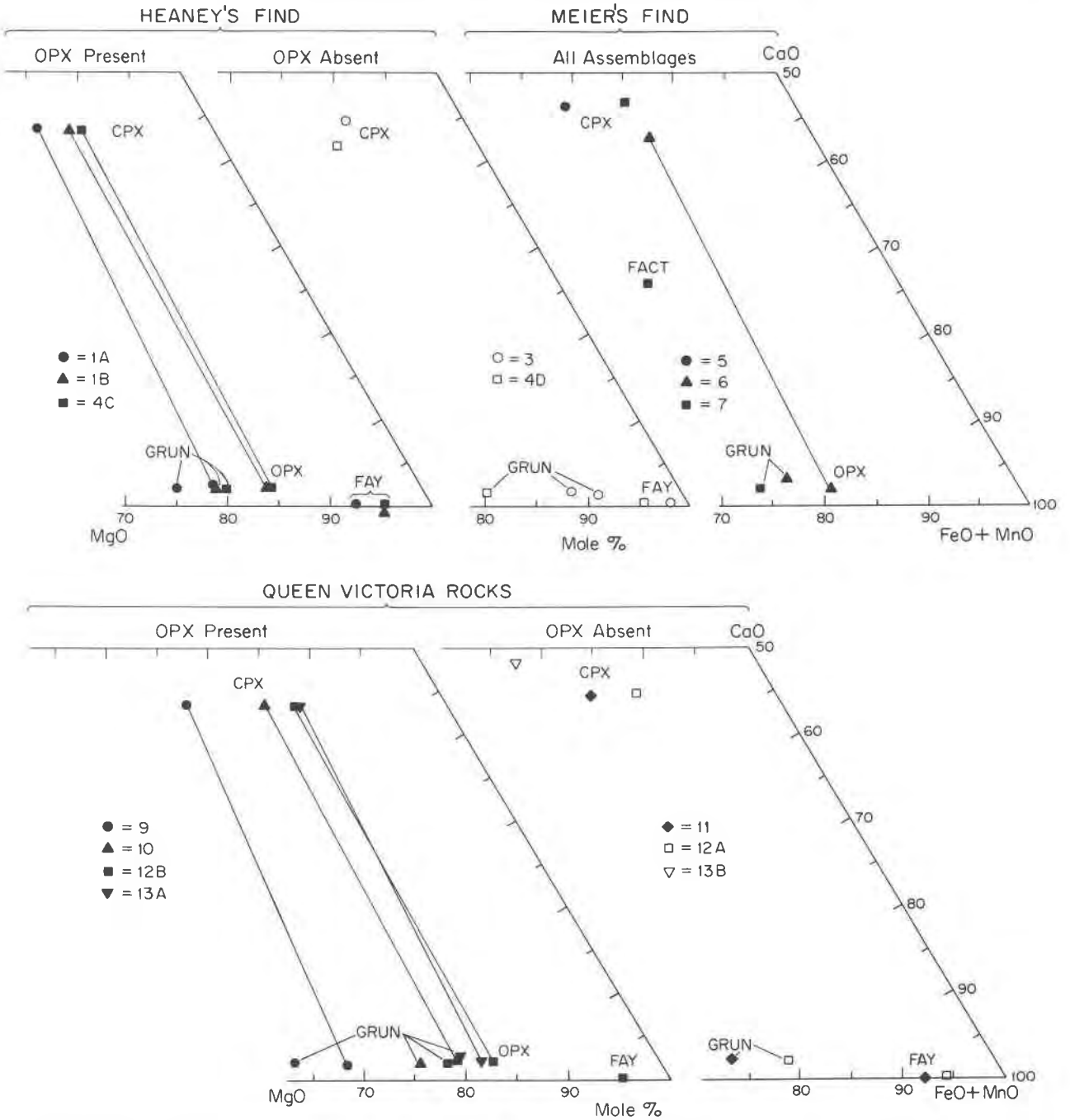

Fig. 3. Graphical representation of electron microprobe analyses of pyroxenes, fayalite, grunerite, and ferroactinolite in iron-formations and Fe-shales. Mineral abbreviations are listed in Table 2. Tie lines join coexisting pyroxene pairs. Total Fe is taken as FeO.

sample 3, which contains the three textural varieties of grunerite described above. Grunerites interpreted to be part of the earliest and somewhat later assemblages (the latter occurs as rims between fayalite and quartz, Fig. 2f) cannot be distinguished by their compositions, suggesting that both crystallized under similar conditions. Fibrous retrograde grunerite is more Fe-rich than the earlier varieties (Table 4, sample 3).

Hornblende shows a wide range of Al^{3+} substitution for Si^{4+} in the tetrahedral site (Table 4). Occupancy of the A site by Na^{+} and K^{+} is highly vari-

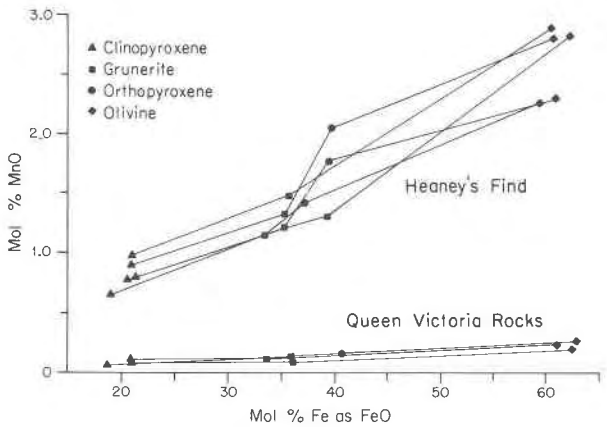

Fig. 4. Mn fractionation in pyroxenes, fayalite, and grunerite. Tie lines join coexisting minerals.

able, although this is greatly influenced by the amount of Fe estimated to be Fe^{3+}. These amphiboles fall within the field of hastingsitic and ferroedenitic hornblende to ferrotschermakitic and ferrohornblende according to the classification of the International Mineralogical Association (Leake, 1978).

Fayalite grains are generally equant, anhedral, and uniform in size (0.2–3.0 mm in diameter, Fig. 2c) within a mesoband, except where they occur as rims on magnetite grains (Fig. 2b; samples 14 and 10). Inclusions consist of quartz and extremely fine-grained magnetite. In several samples, fayalite contains abundant ragged magnetite along fractures and grain boundaries. This magnetite, and perhaps the fine-grained magnetite inclusions, are retrograde in origin. Where fayalite occurs with grunerite or pyroxene, it is only rarely enclosed by these minerals. This is in contrast to fayalite in the metamorphosed Biwabik and Gunflint Iron Formations, where it is commonly mantled by other Fe-silicates (Bonnichsen, 1969, 1975; Morey *et al.*, 1972; Simmons *et al.*, 1974; Floran and Papike, 1978). In the Heaney's Find and Queen Victoria Rocks samples, where fayalite is mantled by grunerite, the latter occurs between fayalite and quartz (Fig. 2f) and rarely between fayalite and hornblende.

Within a single mesoband, fayalite compositions are uniform and independent of the presence or absence of quartz and associated minerals. Fayalite shows a relatively narrow range in Fe/(Fe+Mg) ratios (Table 5). The most Fe-rich fayalite occurs in a very quartz-rich, orthopyroxene-free assemblage (Table 5, no. 3; Fig. 2f). Fayalite contains the highest Mn content of coexisting Fe-silicates (Fig. 4) and the

Table 4. Representative electron microprobe analyses of coexisting and single amphiboles in iron-formations and Fe-shales

	Heaney's Find							Meier's Find			Queen Victoria Rocks					
	3		4C		1B	1A		7		5	12B	13A		13B	14	
wt%	GRUN	GRUN[1]	GRUN	HBLD	GRUN	GRUN	HBLD	GRUN	FACT	HBLD	GRUN	GRUN	HBLD	HBLD	HBLD	CUMM
SiO_2	48.78	49.20	49.78	43.20	49.50	50.70	44.00	50.90	52.00	44.30	49.80	49.97	45.60	48.40	42.20	50.30
TiO_2	0.00	0.04	0.01	0.26	0.00	0.00	0.00	0.00	0.00	0.00	0.00	0.02	0.00	0.04	0.56	0.14
Al_2O_3	0.05	0.02	0.40	8.53	0.22	0.50	7.17	0.11	0.48	8.43	0.49	0.67	6.90	3.68	13.90	2.87
FeO*	43.04	44.60	39.57	29.80	39.00	37.90	28.00	37.40	26.50	24.20	40.30	40.30	28.90	24.10	21.30	27.70
MnO	1.42	1.37	1.47	0.45	1.33	1.29	0.36	1.18	0.43	0.46	0.15	0.21	0.05	0.20	0.08	0.13
MgO	3.11	2.41	5.65	3.68	5.88	7.13	5.08	7.54	7.47	6.90	6.05	5.54	4.22	8.48	8.17	14.20
CaO	0.63	0.49	0.78	10.65	0.79	0.87	10.77	0.94	11.00	11.20	0.86	1.17	10.72	11.76	9.85	1.53
Na_2O	0.00	0.19	0.02	1.44	0.00	0.00	0.37	0.05	0.15	1.23	0.00	0.10	0.72	0.36	1.80	0.52
K_2O	0.00	0.00	0.00	0.96	0.00	0.00	0.83	0.00	0.00	0.83	0.00	0.00	0.07	0.16	0.28	0.00
Total	97.03	98.32	97.68	98.97	96.72	98.39	96.58	98.12	98.03	97.55	97.65	97.98	97.18	97.18	98.14	97.39
Fe_2O_3**	0.00	0.38	0.11	4.70	0.00	0.00	5.99	0.12	0.00	4.42	0.33	0.00	4.55	4.84	7.45	3.76
FeO		44.26	39.48	25.58			22.61	37.29		20.22	40.01		24.81	19.75	14.59	24.66
Total		98.36	97.70	99.45			97.18	98.13		97.99	97.69		97.64	97.67	98.88	98.11
	ions on the basis of 23 oxygens															
Si	8.005	8.003	7.995	6.720	7.975	7.953	6.901	7.985	7.950	6.802	7.934	7.946	7.094	7.362	6.255	7.525
Al	0.000	0.000	0.045	1.280	0.025	0.047	1.009	0.015	0.050	1.198	0.066	0.054	0.906	0.638	1.745	0.475
Σ	8.005	8.003	8.000	8.000	8.000	8.000	8.000	8.000	8.000	8.000	8.000	8.000	8.000	8.000	8.000	8.000
Al	0.010	0.004	0.030	0.285	0.017	0.045	0.226	0.005	0.037	0.327	0.027	0.071	0.360	0.022	0.685	0.031
Ti	0.000	0.005	0.001	0.030	0.000	0.000	0.000	0.000	0.000	0.000	0.000	0.003	0.000	0.005	0.063	0.016
Fe^{3+}	0.000	0.046	0.013	0.550	0.000	0.000	0.707	0.014	0.000	0.511	0.039	0.000	0.532	0.554	0.831	0.380
Fe^{2+}	5.907	6.021	5.275	3.328	5.255	4.968	2.966	4.893	3.388	2.596	5.331	5.359	3.228	2.512	1.809	3.086
Mn	0.197	0.189	0.199	0.059	0.182	0.171	0.048	0.157	0.056	0.060	0.020	0.028	0.007	0.026	0.010	0.017
Mg	0.761	0.584	1.346	0.853	1.412	1.667	1.187	1.763	1.702	1.579	1.437	1.313	0.978	1.922	1.805	3.166
Σ	6.875	6.849	6.864	5.105	6.866	6.851	5.134	6.832	5.183	5.073	6.854	6.774	5.105	5.041	5.203	6.696
X_{VI}	1.875	1.849	1.864	0.105	1.866	1.851	0.134	1.832	0.183	0.073	1.854	1.774	0.105	0.041	0.203	1.696
Ca	0.111	0.085	0.134	1.775	0.136	0.146	1.810	0.158	1.802	1.843	0.147	0.199	1.787	1.917	1.564	0.245
Na_{M4}	0.000	0.060	0.002	0.120	0.000	0.000	0.056	0.010	0.015	0.084	0.000	0.027	0.108	0.042	0.233	0.059
Σ	1.986	1.994	2.000	2.000	2.002	1.997	2.000	2.000	2.000	2.000	2.001	2.000	2.000	2.000	2.000	2.000
Na_A	0.000	0.000	0.003	0.314	0.000	0.000	0.056	0.005	0.029	0.282	0.000	0.004	0.109	0.064	0.284	0.091
K	0.000	0.000	0.000	0.191	0.000	0.000	0.166	0.000	0.000	0.163	0.000	0.000	0.014	0.031	0.053	0.000
Σ	0.000	0.000	0.003	0.505	0.000	0.000	0.222	0.005	0.029	0.445	0.000	0.004	0.123	0.095	0.337	0.091
Total	14.991	14.997	15.003	15.505	15.002	14.997	15.222	15.005	15.029	15.445	15.001	15.004	15.123	15.095	15.337	15.091

*All Fe as FeO. **Fe_2O_3 estimated by the method of Papike et al. (1974). 1. Retrograde. Assemblages listed in Table 2.

most manganiferous fayalite contains more Mn than Mg (Table 5, no. 3).

Magnetite is abundant in quartz-rich assemblages and is a minor constituent of most other iron-formation assemblages. It is a trace constituent of Fe-shale bands. Magnetite is generally finer-grained than the silicates and commonly occurs as inclusions in the Fe-silicates. In the banded iron-formations, it is essentially pure Fe_3O_4. *Ilmenite* occurs with magnetite in several of the Fe-shale bands, where both oxides are minor constituents. In sample 5 ilmenite and magnetite occur as independent and separate grains, whereas in sample 14 they occur as an adjoining pair of intergrown grains that originally may have been a single homogeneous phase. All ilmenite and magnetite have essentially the end-member composition, although magnetite from sample 14 contains 0.12% Al_2O_3 and 0.12% Cr_2O_3 (Table 6). These compositions suggest that the coexisting ilmenite and magnetite equilibrated at temperatures below 500°C (Buddington and Lindsley, 1964). However, the compositions of associated silicates indicate considerably higher metamorphic temperatures (see below) and the low equilibration temperature indicated by the coexisting ilmenite–magnetite is surprising, especially in sample 5 where the oxides occur as isolated grains. Possibly these oxides were not in mutual equilibrium during metamorphism.

Garnet occurs only in Fe-shale bands and is generally subhedral with abundant inclusions. Compositionally it is >60 percent almandine with the remainder mostly grossular, spessartine, and lesser pyrope (Table 7). Garnet compositions are uniform both within single grains and within individual Fe-shale bands.

Biotite also occurs only in Fe-shale bands and is rarely abundant. Biotite and ilmenite, where present, contain most of the TiO_2 (Table 8) reported for the bulk analyses of Fe-shales (Table 1).

Other minerals include apatite, zircon, and pyrrhotite, much of which is altered to marcasite. These minerals generally occur as inclusions in other minerals, although pyrrhotite may form polygonal aggregates with silicates. Plagioclase is present in one Fe-shale band. Greenalite forms rare retrograde veinlets.

The textural relations in the iron-formation and Fe-shale assemblages at Heaney's Find, Meier's Find, and Queen Victoria Rocks indicate that the minerals crystallized together, within the exception of late-stage grunerite and actinolite and retrogade minerals. The primary metamorphic minerals are thus likely to be in chemical equilibrium. Most importantly, the smooth, curved grain boundaries in the eulite–fayalite–quartz-bearing assemblages (samples 1B and 12B) suggest that these are equilibrium assemblages that do not appear to have reequilibrated (except for exsolution phenomena) after they formed, presumably at the peak of metamorphism.

Table 5. Representative electron microprobe analyses of fayalite from Heaney's Find and Queen Victoria Rocks

	Heaney's Find				Queen Victoria Rocks	
wt%	3	4C	1B	1A	12A	11
SiO_2	29.77	30.02	30.10	30.30	29.90	30.60
TiO_2	0.01	0.00	0.01	0.00	0.00	0.01
Al_2O_3	0.00	0.03	0.02	0.02	0.00	0.01
FeO*	65.90	65.04	64.83	64.20	67.50	66.80
MnO	2.98	2.98	2.43	2.41	0.21	0.24
MgO	0.82	1.81	1.86	3.03	2.28	3.10
CaO	0.04	0.04	0.02	0.05	0.04	0.04
Na_2O	0.00	0.00	0.01	0.00	0.00	0.00
K_2O	0.00	0.00	0.00	0.00	0.00	0.00
Total	99.52	99.92	99.28	100.01	99.93	100.80
	ions on the basis of 4 oxygens					
Si	1.005	1.003	1.009	1.002	0.998	1.004
Al	0.000	0.000	0.000	0.000	0.000	0.000
Σ	1.005	1.003	1.009	1.002	0.998	1.004
Al	0.000	0.001	0.001	0.001	0.000	0.000
Fe	1.861	1.817	1.817	1.776	1.884	1.832
Mn	0.083	0.084	0.069	0.068	0.006	0.007
Mg	0.041	0.090	0.093	0.149	0.113	0.152
Ca	0.001	0.001	0.001	0.002	0.001	0.001
Σ	1.986	1.993	1.981	1.996	2.004	1.992

**All Fe as FeO. Assemblages listed in Table 2.*

Table 6. Electron microprobe analyses of coexisting ilmenite and magnetite in Fe-shales from Meier's Find (no. 5) and Queen Victoria Rocks (no. 14)

	5		14	
	ILM	MAG	ILM	MAG
SiO_2	0.14	0.11	0.16	0.17
TiO_2	48.62	0.29	49.32	0.94
Al_2O_3	0.28	0.44	0.12	1.38
Cr_2O_3	0.00	0.08	0.12	4.47
FeO*	45.47	91.64	48.79	86.11
MnO	4.70	0.09	0.15	0.01
MgO	0.00	0.02	0.23	0.16
Total	99.21	92.67	98.89	93.24
Fe_2O_3**	7.05	67.16	5.34	60.17
FeO	39.13	31.21	43.98	31.97
Total	99.92	99.40	99.42	99.27
Mol. % R_2O_3**	3.7		2.7	
Mol. % Ulvö		1.3		4.0

**All Fe as FeO. **Calculated according to the method of Carmichael (1967).*

Discussion and conclusions

Reasonable estimates of the peak metamorphic temperature make it possible to estimate the metamorphic pressure by comparing the composition of

Table 7. Representative electron microprobe analyses of garnet in Fe-shales

	Heaney's Find		Meier's Find	Queen Victoria Rocks
	4B	4A	5	14
SiO_2	37.40	36.50	37.00	37.60
TiO_2	0.00	0.00	0.00	0.00
Al_2O_3	21.20	20.80	20.70	20.80
FeO*	31.30	29.70	28.00	32.50
MnO	4.79	3.87	5.25	0.43
MgO	0.85	0.64	1.93	4.10
CaO	5.08	8.32	7.09	3.62
Na_2O	0.00	0.00	0.00	0.00
K_2O	0.00	0.00	0.00	0.00
Total	100.62	99.83	99.97	99.05
Fe_2O_3**	0.00	0.94	1.11	0.60
FeO		28.85	27.00	31.95
Total		99.92	100.08	99.10
	ions on the basis of 24 oxygens			
Si	6.015	5.914	5.945	6.026
Al	0.000	0.086	0.055	0.000
Σ	6.015	6.000	6.000	6.026
Al	4.019	3.886	3.866	3.930
Ti	0.000	0.000	0.000	0.000
Fe^{3+}	0.000	0.114	0.134	0.070
Σ	4.019	4.000	4.000	4.000
Fe^{2+}	4.210	3.909	3.628	4.283
Mn	0.653	0.531	0.715	0.058
Mg	0.204	0.155	0.462	0.979
Ca	0.875	1.444	1.221	0.622
Σ	5.942	6.039	6.026	5.942
Total	15.976	16.039	16.026	15.968

*All Fe as FeO. **Fe_2O_3 assuming B site = 4.000.

orthopyroxene coexisting with fayalite ± quartz to the experimental data of Smith (1971). Three lines of evidence can be used to constrain the estimate of the peak metamorphic temperature: (a) two-pyroxene geothermometry, (b) orthopyroxene–olivine geothermometry, and (c) the absence of evidence for the crystallization of pigeonite.

The Wood and Banno (1973) geothermometer for coexisting pyroxenes (assumming all Fe as FeO) yields temperatures of 783–803° at Heaney's Find, 805° at Meier's Find, and 790–818°C at Queen Victoria Rocks. The Wells (1977) pyroxene geothermometer yields temperatures of 810–840°, 849°, and 824–871°C for these locations. Ross and Huebner's (1975) graphical geothermometer (Fig. 5) for pyroxene pairs indicates temperatures of approximately 660–720°C for Meier's Find and Queen Victoria Rocks, whereas the pyroxene pairs from Heaney's Find indicate somewhat lower temperatures (~620–650°C). Possible errors introduced by using clinopyroxene compositions that are averages of several single electron probe analyses with a range of 'Wo' contents may mean that the difference in temperature shown in Figure 5 between Heaney's Find and the other two localities is not real. When the pyroxene compositions are corrected for estimated Fe^{3+} contents, both the Wood and Banno and the Wells geothermometers yield marginally higher temperatures (0–5°C higher), whereas the range in temperatures from Ross and Huebner's method is widened slightly (~600°–720°C). Each geothermometer, with the possible exception of Ross and Huebner's, indicates very similar temperatures at all three localities. However, temperatures obtained with the Wells geothermometer are 27–60°C higher than those with the Wood and Banno method, which in turn are considerably higher than those from the Ross and Heubner geothermometer.

Sack (1980) proposed an updated orthopyroxene–olivine geothermometer. This geothermometer (Fig. 6, Sack, 1980) is strictly applicable for 1 atm only, although Sack (personal communication, 1980) sug-

Table 8. Electron microprobe analyses of biotite in Fe-shales

	Heaney's Find	Meier's Find	Queen Victoria Rocks
	4A	5	14
SiO_2	34.92	34.06	35.18
TiO_2	2.03	0.26	2.53
Al_2O_3	15.63	16.70	17.27
FeO*	30.60	26.08	22.04
MnO	0.24	0.36	0.04
MgO	4.00	8.41	10.49
CaO	0.00	0.00	0.10
Na_2O	0.09	0.08	0.53
K_2O	8.17	7.75	6.98
Total	95.68	93.70	95.16
	ions on the basis of 22 oxygens		
Si	5.58	5.44	5.38
Al	2.42	2.56	2.62
Σ	8.00	8.00	8.00
Al	0.53	0.59	0.49
Ti	0.24	0.03	0.29
Fe	4.09	3.49	2.82
Mn	0.03	0.05	0.00
Mg	0.95	2.00	2.39
Σ	5.84	6.16	5.99
Ca	0.00	0.00	0.02
Na	0.03	0.02	0.16
K	1.67	1.58	1.36
Σ	1.70	1.60	1.54
Total	15.54	15.76	15.53

*All Fe as FeO

gests that the method is probably not very sensitive to pressure in the range of 0–8 kbar. $K_{D(Fe-Mg)}$ (OL–OPX) and X_{Fe} (OL) from four eulite–fayalite pairs plotted in Figure 6 of Sack (1980) yield temperatures in the range of approximately 620–700°C. The eulite–fayalite pairs are from samples 14 [$K_{D(Fe-Mg)}$(OL–OPX) = 3.259, X_{Fe}(OL) = 0.923], 1B (3.740, 0.951), and 4C (3.792, 0.953) from Heaney's Find, and sample 12B (3.711, 0.949) from Queen Victoria Rocks.

The absence of pigeonite or orthopyroxene formed by the inversion of pigeonite in the iron-formation assemblages at Heaney's Find, Meier's Find, and Queen Victoria Rocks suggests that the peak metamorphic temperature was below that at which pigeonite forms in very Fe-rich bulk compositions. Relevant experimental data are scarce, but can be used to indicate a probable maximum temperature for the assemblages under discussion. Experimental data pertinent to the formation of pigeonite have recently been reviewed by Ross and Huebner (1979). From their discussion and data, a likely minimum temperature for the formation of pigeonite in bulk compositions having Fe/(Fe+Mg) = 0.75 at 3 kbar is about 800°C. Lindsley *et al.* (1974) determined that at 2.5 kbar the addition of 5 mole percent $MnSiO_3$ to pyroxenes with a bulk composition of Fe/(Fe+Mg) = 0.75 stabilizes pigeonite to about 750°C, or 50° lower than its minimum stability in an Mn-free system. Pyroxenes from Heaney's Find and Meier's Find contain between 2 and a little over 4 mole percent $MnSiO_3$, and their bulk compositions are somewhat more Fe-rich than Fe/(Fe+Mg) = 0.75. The absence of pigeonite from these assemblages thus indicates a maximum metamorphic temperature of 750–800°C. A maximum temperature of about 800°C is indicated at Queen Victoria Rocks, where the $MnSiO_3$ component in pyroxenes is very low (Table 3).

The Ross and Huebner and the orthopyroxene–olivine geothermometers indicate very similar peak metamorphic temperatures. Based on the estimates from these methods the probable metamorphic temperature is 620–720°C, which is consistent with a maximum temperature of 750–800°C indicated by the absence of pigeonite. Other studies have shown that both the Wells and the Wood and Banno geothermometers yield temperatures that are systematically too high, particularly for low-pressure terrains (Bohlen and Essene, 1979; Dahl, 1979; Hewins, 1975; Stormer and Whitney, 1977). Our results support these conclusions.

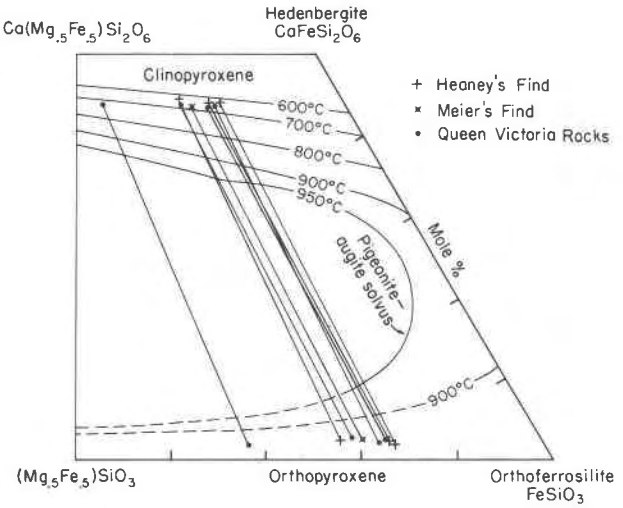

Fig. 5. Coexisting pyroxenes plotted on the two-pyroxene geothermometer of Ross and Huebner (1975).

Applications of the orthopyroxene–olivine-quartz geobarometer of Smith (1971) to natural assemblages requires that the effect of components in addition to Mg, Fe, and Si be considered. The most important additional components are Ca and Mn, which are both partitioned preferentially into orthopyroxene relative to fayalite and which stabilize orthopyroxene instead of olivine + quartz (Bohlen and Essene, 1977; Jaffe *et al.*, 1978; Lindsley *et al.*, 1974; Smith, 1972). Thus, for almost all natural orthopyroxenes the definition of Fs as Fe/(Fe+Mg) will result in an overestimation of pressure when compared to Smith's (1971) data for synthetic orthopyroxene. For the natural orthopyroxenes we have expressed Fs by two different values, Fe/(Fe+Mn+Mg) and Fe/(Fe+Mn+Mg+Ca), in an attempt to take account of the presence of Mn and Ca in a similar although slightly different manner to Jaffe *et al.* (1978). The resulting Fs values for two eulites coexisting with fayalite and quartz bracket a small pressure range at 620–720°C (Fig. 6). The pressure derived for the orthopyroxene from Queen Victoria Rocks, which is Mn-poor [Mn/(Fe+Mn+Mg) = 0.003], is slightly higher than for the Mn-bearing eulite [Mn/(Fe+Mn+Mg) = 0.037] from Heaney's Find.

A minimum pressure estimate can be obtained from the orthopyroxene-bearing but olivine-free assemblages at Meier's Find (sample 6). Eulite from these assemblages is Mn-bearing [Mn/(Fe+Mn+Mg) = 0.025], and its Fs values [Fe/(Fe+Mn+Mg) = 0.787, Fe/(Fe+Mn+Mg+Ca) = 0.769] yield pressures about 1 kbar lower than those indicated by the Heaney's Find eulite, which is also Mn-bearing.

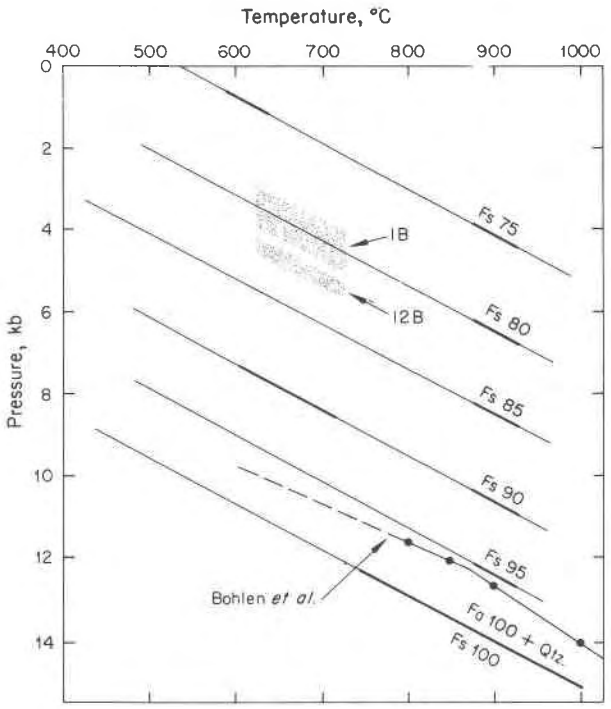

Fig. 6. *P-T* diagram (after Jaffe *et al.*, 1978) with isopleths showing the composition of orthopyroxene coexisting with olivine and quartz, based on experimental work in the MgO–FeO–SiO_2 system by Lindsley (1965) and Smith (1971). The Fs_{100} isopleth determined by Bohlen *et al.* (1978) is also shown. The shaded areas bracket the estimated metamorphic temperature ranges. The Fs values were calculated as Fe/(Fe+Mn+Mg) (upper boundary) and Fe/(Fe+Mn+Mg+Ca) (lower boundary) for eulites from Heaney's Find (1B) and Queen Victoria Rocks (12B).

The difference in pressures indicated by eulite compositions from Heaney's Find (and perhaps Meier's Find) and Queen Victoria Rocks may, however, not be real, or at least not as large as indicated in Figure 6, because Mn is treated as having the same pressure-lowering effect as Mg in the calculation of the Fs values. This is unlikely. The effect of Mn should be less than that of Mg because in the Heaney's Find and Queen Victoria Rocks assemblages Mn [$K_{D(Fe-Mn)}$(OL–OPX) = 1.00–1.19] is fractionated less than Mg [$K_{D(Fe-Mg)}$(OL–OPX) = 3.26–3.79] between fayalite and eulite (see also Berg, 1977; Jaffe *et al.*, 1978). The Fs values we have used should thus yield pressures that are somewhat low.

A further uncertainty in using the orthopyroxene–olivine–quartz geobarometer is introduced by the discrepancy between the position of Smith's (1971) and Bohlen *et al.*'s (1978) *P-T* curve for the reaction $Fs_{100} = Fa_{100} + Qtz$ (Fig. 6). Bohlen *et al.*'s data suggest that the Fs_{100} isopleth should be almost 1 kbar lower at 700°C than that of Smith. If all Fs isopleths are lowered by a similar amount, then the shaded areas in Figure 6 would be correspondingly lower.

The *P-T* conditions (670±50°C, 3–5 kbar) depicted in Figure 6 for Heaney's Find and Queen Victoria Rocks are similar to those estimated for the high-grade regional terrains in the Eastern Goldfields Province of the Yilgarn Block (Binns *et al.*, 1976; Binns and Groves, 1976). Lower pressures, as perhaps required by the experimental data of Bohlen *et al.* (1978), are, however, also consistent with the geology at these localities and would indicate a relatively high thermal gradient during metamorphism.

Acknowledgments

We thank Spargos Exploration N.L. for permission to sample diamond drill core from Queen Victoria Rocks. Part of this study was undertaken while M.J.G. held a Commonwealth Postgraduate Research Award at the University of Western Australia. Further funding was provided by NSF grant EAR 76-11740 (to C.K.). The electron microprobe used in the study was obtained on NSF grant GA-37109 (to C.K.), with joint funds from the Indiana University Foundation. We thank W. H. Moran, R. T. Hill, and J. R. Tolan for the drafting of the illustrations; Mrs. Thea Brown for the typing of the manuscript; D. Weaver for his upkeep of the electron microprobe; and R. A. Binns and R. F. Floran for their critical review of the manuscript and their constructive comments.

References

Albee, A. L. and Ray, L. (1970) Correction factors for electron probe microanalyses of silicates, oxides, carbonates, phosphates, and sulfates. Analytical Chemistry, 42, 1408–1419.

Archibald, N. J. and Bettenay, L. F. (1977) Indirect evidence for tectonic reactivation of a pre-greenstone sialic basement in Western Australia. Earth and Planetary Science Letters, 33, 370–378.

Archibald, N. J., Bettenay, L. F., Binns, R. A., Groves, D. I. and Gunthorpe, R. J. (1978) The evolution of Archean greenstone terrains, Eastern Goldfield's Province, Western Australia. Precambrian Research, 6, 103–131.

Arriens, P. A. (1971) The Archean geochronology of Australia. Geological Society of Australia Special Publication, 3, 11–23.

Baxter, J. L. (1965) Petrology of a banded iron-formation, Koolanooka Hills, Western Australia. B.Sc. (Hons.) Thesis, University of Western Australia, Perth.

Bence, A. E. and Albee, A. L. (1968) Empirical correction factors for the electron microanalysis of silicates and oxides. Journal of Geology, 76, 382–403.

Berg, J. H. (1977) Regional geobarometry in the contact aureoles of the anorthositic Nain Complex, Labrador. Journal of Petrology, 18, 399–430.

Binns, R. A. and Groves, D. I. (1976) Iron–nickel partition in metamorphosed olivine–sulfide assemblages from Perseverance, Western Australia. American Mineralogist, 61, 782–787.

Binns, R. A., Gunthorpe, R. J., and Groves, D. I. (1976) Metamorphic patterns and development of greenstone belts in the Eastern Yilgarn Block, Western Australia. In B. F. Windley, Ed., The Early History of the Earth, p. 303–313. Wiley, London.

Bohlen, S. R. and Essene, E. J. (1977) Errors in applying OPX-

OLIV-QTZ barometry. (abstr.) Transactions of the American Geophysical Union, 58, 1242.

Bohlen, S. R. and Essene, E. J. (1979) A critical evaluation of two-pyroxene thermometry in Adirondack granulites. Lithos, 12, 335–345.

Bohlen, S. R., Boettcher, A. L. and Essene, E. J. (1978) Experimental reinvestigation of ferrosilite–fayalite–quartz stability. (abstr.) Transactions of the American Geophysical Union, 59, 402.

Bonnichsen, B. (1979) Metamorphic pyroxenes and amphiboles in the Biwabik Iron Formation, Dunka River Area, Minnesota. Mineralogical Society of America Special Paper, 2, 217–239.

Bonnichsen, B. (1975) Geology of the Biwabik Iron Formation, Dunka River Area, Minnesota. Economic Geology, 70, 319–340.

Buddington, A. F. and Lindsley, D. H. (1964) Iron–titanium oxide minerals and synthetic equivalents. Journal of Petrology, 5, 310–357.

Carmichael, I.S.E. (1967) The iron–titanium oxides of sialic volcanic rocks and the associated ferromagnesian silicates. Contributions to Mineralogy and Petrology, 14, 36–64.

Dahl, P. S. (1979) Comparative geothermometry based on major-element and oxygen isotope distributions in Precambrian metamorphic rocks from southwestern Montana. American Mineralogist, 64, 1280–1293.

Floran, R. J. and Papike, J. J. (1978) Mineralogy and petrology of the Gunflint Iron Formation, Minnesota–Ontario: correlation of compositional and assemblage variations at low to moderate grade. Journal of Petrology, 19, 215–288.

Gole, M. J. (1980a) Low-temperature retrograde minerals in metamorphosed Archean banded iron-formations, Western Australia. Canadian Mineralogist, 18, 205–215.

Gole, M. J. (1980b) Metamorphosed banded iron-formations in the Archean Yilgarn Block, Western Australia. Economic Geology, in press.

Haase, C. S. and Klein, C. (1978) Paragenesis of olivine in the regionally metamorphosed Negaunee Iron-Formation, Republic Mine, Northern Michigan. (abstr.) Geological Society of America Abstracts with Programs, 10, 414.

Hewins, R. H. (1975) Pyroxene geothermometry of some granulite facies rocks. Contributions to Mineralogy and Petrology, 50, 205–209.

Immega, I. P. and Klein, C. (1976) Mineralogy and petrology of some metamorphic Precambrian iron-formations in south-western Montana. American Mineralogist, 61, 1117–1144.

Jaffe, H. W., Robinson, P. and Tracy, R. J. (1978) Orthoferrosilite and other iron-rich pyroxenes in microperthite gneiss of the Mount Marcy area, Adirondack Mountains. American Mineralogist, 63, 1116–1136.

Leake, B. E. (1978) Nomenclature of amphiboles. American Mineralogist, 63, 1023–1052.

Lindsley, D. H. (1965) Ferrosilite. Carnegie Institution of Washington Year Book, 64, 148–150.

Lindsley, D. H., Tso, J. and Heyse, J. V. (1974) Effect of Mn on the stability of pigeonite. (abstr.) Geological Society of America Abstracts with Programs, 6, 846–847.

Miles, K. R. (1943) Grunerite in Western Australia. American Mineralogist, 28, 25–38.

Miles, K. R. (1946a) Geological notes on boring in the Mt. Palmer District, Yilgarn Goldfield. Geological Survey of Western Australia Annual Report 1945, 43–46.

Miles, K. R. (1946b) Metamorphism of the jasper bars of Western Australia. Quarterly Journal of the Geological Society, 102, 115–155.

Morey, G. B., Papike, J. J., Smith, R. W. and Weiblen, P. W. (1972) Observations on the contact metamorphism of the Biwabik Iron Formation, East Mesabi District, Minnesota. Geological Society of America Memoir, 135, 225–263.

Papike, J. J., Cameron, K. L. and Baldwin, K. R. (1974) Amphiboles and pyroxenes: characterizations of *other* than quadrilateral components and estimates of ferric iron from microprobe data. (abstr.) Geological Society of America Abstracts with Programs, 6, 1053–1054.

Ross, M. and Huebner, J. S. (1975) A pyroxene geothermometer based on composition–temperature relationships of naturally occurring orthopyroxene, pigeonite and augite. Extended abstract, International Conference on Geothermometry and Geobarometry, Pennsylvania State University.

Ross, M. and Huebner, J. S. (1979) Temperature–composition relationships between naturally occurring augite, pigeonite, and orthopyroxene at one bar pressure. American Mineralogist, 64, 1133–1155.

Sack, R. O. (1980) Some constraints on the thermodynamic mixing properties of Fe–Mg orthopyroxenes and olivines. Contributions to Mineralogy and Petrology, 71, 257–269.

Simmons, E. C., Lindsley, D. H. and Papike, J. J. (1974) Phase relations and crystallization sequence in a contact-metamorphosed rock from the Gunflint Iron Formation, Minnesota. Journal of Petrology, 15, 539–565.

Smith, D. (1971) Stability of the assemblage iron-rich orthopyroxene–olivine–quartz. American Journal of Science, 271, 370–382.

Smith, D. (1972) Stability of iron-rich pyroxene in the system $CaSiO_3$–$FeSiO_3$–$MgSiO_3$. American Mineralogist, 57, 1413–1428.

Stormer, J. C. and Whitney, J. A. (1977) Two-feldspar geothermometer in granulite facies metamorphic rocks. Contributions to Mineralogy and Petrology, 65, 123–133.

Wells, P. R. A. (1977) Pyroxene thermometry in simple and complex systems. Contributions to Mineralogy and Petrology, 62, 129–139.

Wood, B. J. and Banno, S. (1973) Garnet–orthopyroxene and orthopyroxene–clinopyroxene relationships in simple and complex systems. Contributions to Mineralogy and Petrology, 42, 109–124.

Manuscript received, April 24, 1980;
accepted for publication, August 18, 1980.